

## DNA compaction: fundamentals and applications

André Estévez-Torres<sup>a</sup> and Damien Baigl<sup>\*bcd</sup>

Received 3rd March 2011, Accepted 5th April 2011

DOI: 10.1039/c1sm05373f

Compaction is the process in which a large DNA molecule undergoes a transition between an elongated conformation and a very compact form. In nature, DNA compaction occurs to package genomic material inside tiny spaces such as viral capsids and cell nuclei. *In vitro*, several strategies exist to compact DNA. In this review, we first provide a physico-chemical description of this phenomenon, focusing on the modes of compaction, the types of compaction agents and the chemical and physical parameters that control compaction and its reverse process, decompaction. We then describe three main kinds of applications. First, we show how regulated compaction/decompaction can be used to control gene activity *in vitro*, with a particular emphasis on the use of light to reversibly control gene expression. Second, we describe several approaches where compaction is used as a way to reversibly protect DNA against chemical, biochemical, or mechanical stresses. Third, we show that compact DNA can be used as a nanostructure template to generate nanomaterials with a well-defined size and shape. We conclude by proposing some perspectives for future biochemical and biotechnological applications and enumerate some remaining challenges that we think worth being undertaken.

### 1. Introduction

Less than 60 years after the description of the DNA double-helix structure,<sup>1</sup> DNA has become a very familiar molecule. In the news, DNA is used to identify criminals or to assess the authenticity of a piece of hair. In cinema pictures, it is used to resurrect dinosaurs or to create avatars. In laboratories, DNA is amplified by biochemists, stretched by physicists, modified by chemists. With the opening era of personal genomics, DNA is

<sup>a</sup>Laboratoire de photonique et de nanostructures, LPN-CNRS, route de Nozay, 91460 Marcoussis, France. E-mail: aestevez@lpa.cnrs.fr

<sup>b</sup>Department of Chemistry, Ecole Normale Supérieure, 75005 Paris, France. E-mail: damien.baigl@ens.fr; Fax: +33 1 4432 2402; Tel: +33 1 4432 2405

<sup>c</sup>Université Pierre et Marie Curie Paris 6, 75005 Paris, France  
<sup>d</sup>UMR 8640, CNRS, France



André  
Estévez-Torres

André Estévez-Torres was born in Vigo, Spain. He obtained a MSc in chemistry and physics in 2003 at Ecole normale supérieure, Paris and a PhD in chemistry in 2007 working with Prof. Ludovic Jullien at Université Pierre et Marie Curie in Paris. He then spent a year at the Department of Physics at Kyoto University and two years at Princeton University, working, respectively, with Profs. Kenichi Yoshikawa and Robert H. Austin. He has recently moved to the Laboratoire de photonique et de nanostructures in Marcoussis, France, where he carries out research on the engineering of chemical dynamic systems.



Damien Baigl

Damien Baigl is a professor at UPMC and group leader at the Department of Chemistry of Ecole Normale Supérieure (ENS) in Paris. He did a PhD under the supervision of C. E. Williams in the laboratory of P.-G. de Gennes at College de France (2001–2003) and a post-doc in the group of K. Yoshikawa at Kyoto University (2003–2005). He is now developing bottom-up physico-chemical approaches to understand and control complex and biological systems. His research interests include DNA compaction, photocontrol of gene expression, artificial cell models, microfluidics for cell and systems biology, and photo-actuation of micro- and macrofluidic systems.

also the cornerstone of great economical and health challenges. The aim of this review is therefore not to unveil unknown aspects, if any, of DNA neither to make an exhaustive enumeration of experimental results, theoretical considerations, and numerical simulations on DNA but to present in a concise way one phenomenon, DNA compaction, from a physico-chemical point of view and to stress out some potential applications as diverse as nanomaterials fabrication, DNA manipulation, and gene regulation.

In living cells, genomic DNA is a long, highly charged, and rather stiff polymer that has to undergo a strong compaction process to fit within tiny available spaces (*e.g.*, the nucleus in eukaryotic cells). This process, also called DNA condensation, can be reproduced and studied *in vitro*. Several particularly interesting review articles have been published in this field. 'DNA-inspired electrostatics' is a short review describing in accessible words delicate physical concepts (such as like-charged attraction) involved in DNA compaction.<sup>2</sup> Both physical and biochemical aspects of DNA compaction have been remarkably summarized by Bloomfield.<sup>3,4</sup> Ref. 5 is a detailed review on DNA compaction/decompaction strategies. Ref. 6 focuses on the nanostructure organization of compacted DNA. The application of DNA compaction in gene delivery, which is of great importance for the success of gene therapy protocols, is well documented in the literature<sup>7</sup> and it is out of the scope of this review. Herein, we shall give a brief physico-chemical description of *in vitro* DNA compaction (modes of DNA compaction, compaction agents, reversibility) before discussing three selected applications: gene regulation (DNA conformation as a trigger of biochemical switches), DNA manipulation (compaction as a protection strategy), and nanostructure fabrication (compact DNA as a nanostructure template).

## 2. *In vitro* DNA compaction and decompaction

### 2.1. Physico-chemical ID of a familiar molecule

Double-stranded DNA is organized into a double-helical structure with a diameter  $d = 2$  nm. Each base pair (bp) has a size  $a = 0.34$  nm and possesses two negatively charged phosphate groups, corresponding to an average distance between charges  $b = 0.17$  nm. DNA persistence length  $l_p$ , which is of the order of 50 nm (about 150 bp), provides a local stiffness to the molecule.<sup>8</sup> To each phosphate group corresponds a cationic counter-ion, which can be free in solution or electrostatically interacting with the DNA molecule. In the framework of the Manning–Oosawa condensation theory,<sup>9</sup> a fraction of counter-ions localize in the vicinity of the DNA chain to decrease the electrostatic potential created along the highly charged chain. In average, one DNA phosphate group remains effectively charged every Bjerrum length,  $l_B$ , the distance at which the electrostatic energy between two elementary charges equals  $k_B T$  ( $l_B = e^2/(4\pi\epsilon k_B T)$  with  $e$  the elementary charge,  $\epsilon$  the solvent dielectric constant,  $k_B$  the Boltzmann constant,  $T$  the temperature). In the case of counter-ions having a valency  $Z$ , for a same entropic cost, the neutralization is  $Z$ -fold more effective and the distance between effectively charged DNA monomers becomes  $Zl_B$ . The fraction of effectively charged DNA monomers is thus  $f_{\text{eff}} = b/(Zl_B)$  and the neutralization rate is  $\theta = 1 - f_{\text{eff}} = 1 - b/(Zl_B)$ . For instance, in

pure water at 25 °C,  $l_B = 0.71$  nm and  $\theta = 0.76, 0.88, 0.92$ , and 0.94, for  $Z = 1, 2, 3$ , and 4, respectively. These figures indicate that over 75% of DNA phosphate groups are neutralized by DNA monovalent counter-ions and that this neutralization significantly increases with an increase in  $Z$ . The Manning–Oosawa condensation theory, although obtained from a quite unrealistic case (an infinitely long charged rod) and still strongly debated, has the advantage to provide essential physical ingredients as well as a good estimate of the effective charge of a DNA molecule.

For this review, we shall mainly focus on long genomic DNA molecules (significantly larger than  $l_p$ ) in a dilute solution, that is, DNA molecules are not concentrated in the solution and have few interactions between each other. The compaction will thus be unimolecular (that is, involving one DNA molecule) and will result from intramolecular DNA monomer–monomer attractions, usually induced by the addition of an appropriate compaction agent. In such case, the compaction behaviour will be essentially independent of the DNA chain length.

### 2.2. Three modes for DNA compaction

In water solution, DNA adopts an elongated coil conformation due to the strong repulsion between negatively charged phosphate groups. Upon addition of appropriate compaction agents (see Section 2.3), DNA undergoes a strong compaction process. The identification of the modes of compaction was possible thanks to the remarkable contribution of the Yoshikawa group who brought the analysis of DNA compaction at the level of individual molecules. Fig. 1 shows three pathways that can be followed by DNA to go from the elongated coil state to the compact state. The first type is an all-or-none compaction process where there is no intermediate state but coexistence between the elongated coil state and the compact state.<sup>10,11</sup> This process is usually observed when attraction is induced between DNA monomers all along the chain, either by adding small multi-valent counter-ions or by inducing unfavorable contacts between DNA monomers and the solvent (*e.g.*, addition of a poor solvent such as ethanol or addition of neutral polymers that exclude volume to DNA). This is similar to the first-order phase transition between a disordered gas phase (coil state) and a highly condensed solid phase (compact state).<sup>11</sup> The second

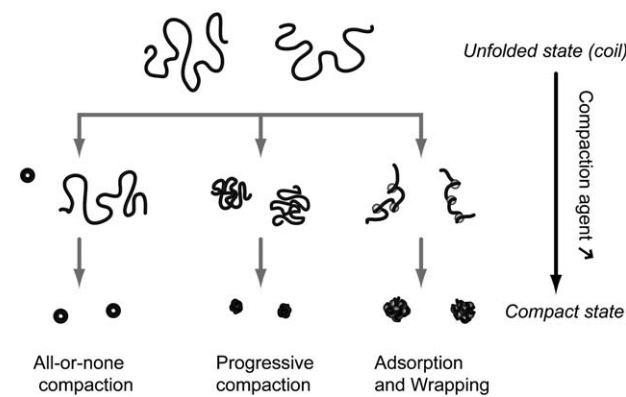


Fig. 1 Schematic representation of the 3 principal modes of *in vitro* unimolecular DNA compaction.

mode of compaction is a progressive transition from the elongated coil state to the compact state. This usually occurs when a strong attraction between several consecutive DNA monomers can be induced locally, typically upon complexation with polycations longer than 10 monomers.<sup>12</sup> The two precedent modes of compaction account for a collapse of DNA resulting from DNA monomer–monomer attractive interactions. The highly packaged structure of DNA inside viruses probably results from a combination of these two modes. The third possible route is an assisted, hierarchical compaction by DNA adsorption and wrapping around nanoscale objects. This is the mode of compaction of DNA into chromatin in eukaryotic cells and it is observed *in vitro* when DNA is compacted by cationic nanoparticles<sup>13,14</sup> or dendrimers.<sup>15</sup> Clearly, other pathways are possible and intermediate routes between the three cases shown in Fig. 1 are usually observed. For example, DNA compaction by cationic surfactants proceeds through the coexistence between DNA in the fully compact state and DNA shrunk coils, indicating an intermediate route between an all-or-none transition and a progressive compaction.<sup>16,17</sup> Segregated states, where the same DNA molecule is composed of compact and unfolded parts, can also be observed under specific conditions.<sup>18,19</sup>

### 2.3. Compaction agents

Compaction agents are molecules that can induce DNA monomer–monomer attraction and/or provoke unfavorable interaction between DNA and the solvent.

**(1) General considerations on multivalent counter-ions.** DNA monomer–monomer attraction can be induced by addition of multivalent counter-ions. The accumulation of multivalent ions near the vicinity of the DNA chain by ion exchange with DNA counter-ions can induce DNA monomer–monomer attraction through the correlation of counter-ion fluctuations. It is important to note that neutralization is not directly responsible for DNA compaction but it can be used as a phenomenological parameter to estimate the onset of DNA compaction. It has been experimentally observed that for many types of counter-ions and a wide range of experimental conditions (different salt concentrations and dielectric constants), DNA compaction occurs when the neutralization rate reaches  $\theta \approx 0.89$ .<sup>20–22</sup> According to the simple Manning–Oosawa condensation mechanism described in the first section, this indicates that counter-ions with valencies  $Z = 1$  and  $2$  ( $\theta = 0.76$  and  $0.88$ , respectively) cannot induce DNA compaction. In contrast, cationic species with  $Z \geq 3$  can favourably exchange with DNA condensed counter-ions and induce sufficient neutralization to provoke DNA compaction. These simple considerations clearly indicate that multi-valent species with a higher valency will be more prone to induce DNA compaction, *i.e.*, a smaller concentration of condensation agent will be necessary to induce DNA compaction.

**(2) Small multi-valent counter-ions.** The most commonly used multi-valent counter-ions with  $Z \geq 3$  are naturally occurring polyamines such as spermidine (3+ at pH = 7)<sup>11,23</sup> and spermine (4+ at pH = 7),<sup>20,22,24</sup> and the inorganic cation  $\text{Co}(\text{NH}_3)_6^{3+}$ .<sup>25,26</sup>

Other metal cations such as  $\text{Al}^{3+}$  (ref. 27 and 28), lanthanide ions ( $\text{La}^{3+}$ ,  $\text{Eu}^{3+}$ ,  $\text{Tb}^{3+}$ ) (ref. 29),  $\text{Ga}^{3+}$  (ref. 28),  $\text{Cr}^{3+}$  (ref. 30) and

$\text{Fe}^{3+}$  (ref. 31) have also been used. In most cases, these multivalent counter-ions induce an all-or-none compaction.<sup>10,11,31</sup> Since these multivalent counter-ions are in competition with mono-valent salts present in the medium, an excess of condensing agent is necessary to induce DNA compaction. The critical compaction agent over DNA charge ratio to induce full compaction,  $\rho^*$ , is thus much larger than 1 (Fig. 2). For similar reasons,  $\rho^*$  increases with an increase in the concentration of low valence salts (mono-valent or valency smaller than  $Z$ ) present in the medium.<sup>20</sup> Conversely, since neutralization becomes more effective for higher  $Z$ ,  $\rho^*$  strongly decreases with an increase in  $Z$  to reach  $\rho^* \approx 1$  for approximately  $Z \approx 10$  (Fig. 2).<sup>12</sup>

**(3) Linear polycations.** For  $Z > 10$ , compaction agents can be considered as long polycations. Typical examples of polycations are polyethyleneimine and cationic polypeptides such as polylysine.<sup>32</sup> When these polycations are added into a DNA solution, they strongly interact with DNA to form interpolyelectrolyte complexes whose formation is favoured by the release of condensed counter-ions from both DNA and the polycation. Each added molecule can induce a local DNA collapse,<sup>33</sup> which explains that this compaction is usually progressive from the elongated coil state to the compact state, which is typically reached for  $\rho^* \approx 1$  regardless of  $Z$  (Fig. 2). The valency of the compaction agent has thus a critical role in determining the nature of the compaction as well as the characteristic concentration necessary to induce compaction. This effect is summarized in Fig. 2. For small  $Z$  values ('multi-valent counter-ions'), the transition is all-or-none, it strongly depends on  $Z$ , and a large excess of compaction agent is necessary to induce full compaction. For large  $Z$  values ('long polycations'), the compaction is progressive and occurs at  $\rho^* \approx 1$  regardless of  $Z$ . The transition zone strongly depends on the chemical nature of the compaction agent as well as on the concentration of other salts present in the medium; it typically occurs for  $Z$  in the range 5–10.<sup>12</sup>

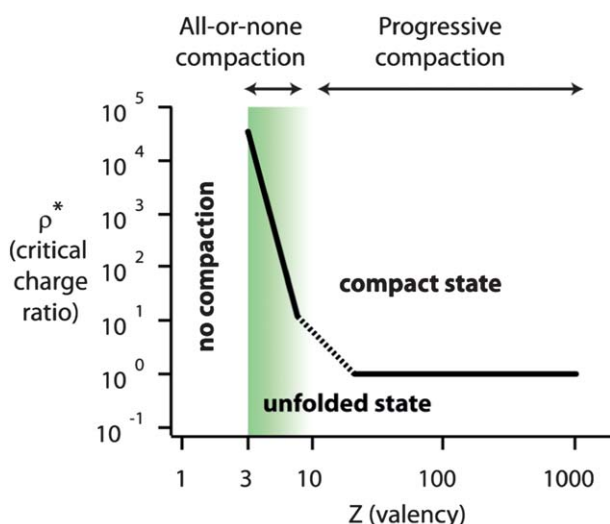


**Fig. 2** Schematic representation of the mode of compaction (all-or-none or progressive) and critical compaction agent over DNA charge ratio necessary to induce full compaction ( $\rho^*$ ) as a function of the valency of the compaction agent ( $Z$ ) in the case of purely electrostatic interactions. Inspired from ref. 12.

**(4) Tridimensional polycationic nanostructures.** Highly charged, multivalent cationic species with supramolecular dimensions, such as cationic dendrimers,<sup>15,34</sup> supramolecular assemblies,<sup>35</sup> and nanoparticles,<sup>13,14</sup> can also induce DNA compaction. Due to the local rigidity of DNA (the persistence length is 50 nm), the mode of compaction strongly depends on the 3D spatial arrangement of charges and on the flexibility of the compaction agent. Under appropriate conditions, DNA compaction proceeds by adsorption and wrapping (Fig. 1) in a way similar to DNA packaging in chromatin<sup>13,14</sup> but other pathways are possible. For instance, in the case of cationic nanoparticles, three modes of compaction have been identified as a function of nanoparticle size: DNA adsorption on large nanoparticles; DNA wrapping on nanoparticles of intermediate dimensions; and adsorption of nanoparticles on the DNA chain for very small nanoparticles.<sup>14</sup> The characteristic sizes delimiting the transition between these compaction modes significantly decrease with an increase in nanoparticle cationic charge. These results show the delicate interplay between electrostatic interactions and molecular rigidity of DNA in the control of the hierarchical packaging of DNA into chromatin. The hierarchical packaging of DNA into chromatin can be reproduced *in vitro* by compacting DNA with histone proteins. DNA compaction can also be achieved by histones H1 and H5.<sup>36,37</sup>

**(5) Amphiphilic cationic species (surfactants).** Fig. 2 shows that DNA compaction by multivalent species is only possible for  $Z \geq 3$ . This holds true as long as compaction agents only interact as individual species through sole electrostatic interactions. When compaction agents contain some hydrophobic parts and/or have ability to self-assemble, hydrophobicity and cooperative effects have to be taken into account. Cationic surfactants are the most usual compaction agents that can be classified in this category.<sup>16,17</sup> Since the pioneering works of Hayakawa, it has been well established that the binding of cationic surfactants to DNA is highly cooperative.<sup>38</sup> Therefore, any physico-chemical parameter that promotes surfactant aggregation enhances the ability of the surfactant molecules to cooperatively bind to DNA and therefore favours DNA compaction at a lower surfactant concentration. This enhancement of compaction ability is observed when the hydrophobicity of the apolar tail is increased<sup>39,40</sup> or when a co-solute that favours surfactant aggregation is added, such as negatively charged polyelectrolytes or nanoparticles.<sup>41</sup>

**(6) Neutral and anionic polymers.** In all of the above-mentioned examples, DNA compaction was achieved by the interaction between negatively charged phosphate groups of DNA and one or several compounds of opposite charge. Another possibility is to induce unfavourable contacts between DNA monomers and the solvent. This can be achieved by adding ethanol<sup>42</sup> or decreasing the dielectric constant of the solvent.<sup>43</sup> Another possibility is to add another water soluble polymer, which can be neutral such as polyethyleneglycol (PEG),<sup>44,45</sup> or anionic such as polyaspartate, polyglutamate, and anionic polypeptides.<sup>46</sup> A high concentration of these species ('crowding agents') excludes volume to DNA and induces DNA compaction. Since DNA compaction results from a global collapse of the

DNA chain, the folding transition is usually all-or-none at the single-molecule level.<sup>45</sup>

#### 2.4. Compact state: size, shape and stability

The shape of the compacted DNA results from a balance between surface energy and DNA rigidity. This last parameter can be modified through the addition of monovalent salts yielding larger DNA condensates.<sup>47</sup> A toroid with a diameter twice the persistence length is the most common shape,<sup>6,23,48</sup> although spherical globules<sup>49</sup> are also frequent, and rods,<sup>50</sup> flowers<sup>51</sup> and racket-shaped<sup>52</sup> condensates have also been reported. For DNAs shorter than 40 kbp, single toroids are obtained upon compaction with multivalent cations and their internal diameter decreases with increasing DNA length. Beyond this length, multiple toroids are formed from a single DNA molecule.<sup>55</sup>

The formation of the compact state is counterintuitive for two reasons. First, it is surprising to obtain a stable and dense condensate of a highly charged object (at the onset of compaction DNA still bears 10% of its original charge). Second, it is remarkable that the condensates display a well-defined size. The stability of the compact state is explained in Bloomfield's review.<sup>56</sup> Three repulsive contributions to the total free energy need to be considered: (i) bending, coming from the intrinsic rigidity of dsDNA and accounting for  $\sim +1/300 k_B T$  per bp; (ii) entropic demixing of polymer and solvent, evaluated to  $+1/150 k_B T$  per bp;<sup>57</sup> and (iii) electrostatic repulsion, estimated using Oosawa's framework<sup>9</sup> to be  $+0.24 k_B T$  per bp. Electrostatic attractive interactions are ruled out in the framework of Debye–Hückel and Poisson–Boltzmann descriptions and one needs to consider correlated counterion fluctuations at short distances that are estimated to be  $-0.3 k_B T$  per bp.<sup>58</sup> Adding up repulsive and attractive contributions, the free energy of the compact state is of the order of  $-0.05 k_B T$  per bp, or  $-0.1 \text{ kJ (mol of bp)}^{-1}$ , compatible with a stable compact state.

Two possible causes have been evoked to explain the limited-size of DNA condensates.<sup>59</sup> The first one, thermodynamic, calls for a repulsive free energy coming from topological defects intrinsic to the winding of a linear polymer inside a toroid. The second, kinetic, arises from the energy barrier that two randomly oriented charged rods have to overcome to attain the parallel, attractive, configuration at small separations; a barrier that increases with the size of the condensate. Both contributions become more positive with an increase in toroid size, which could explain the limited size of DNA condensates. Experimentally, toroids have been typically reported to measure around 90–100 nm, which is slightly smaller than  $2l_p$ . This value mainly depends on the salt concentration<sup>47</sup> and the presence of nucleation loops.<sup>47,60</sup> While compaction agent concentration has usually a minor effect on the size of the compact state, it was shown to significantly affect the size of DNA globules and toroids in the case of polyethyleneimine as a compaction agent.<sup>61</sup>

The first observation of a toroid-like DNA condensate was reported by electron microscopy by Gosule and Schellman in 1976 using spermidine as a condensing agent<sup>23</sup> and it was later described in exquisite detail by Hud and coworkers<sup>47,48</sup> (Fig. 3A), showing that, in some of the toroids, DNA is hexagonally packed with an interchain distance of 2.6 nm. A related structure has

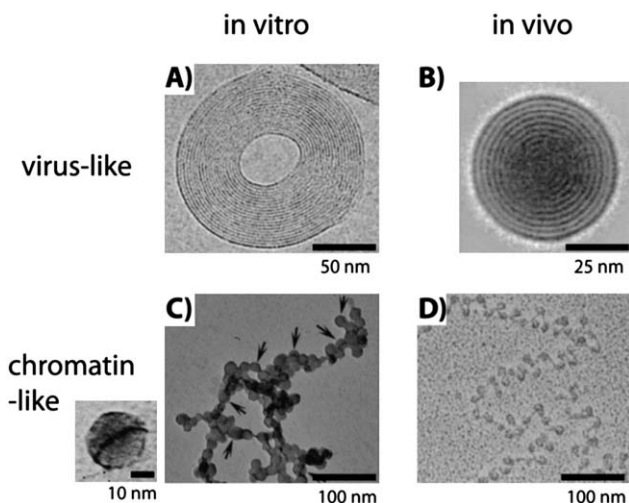


**Fig. 3** Comparison of *in vitro* and *in vivo* structures of compacted DNA observed by transmission electron microscopy. (A) Cryoelectron image of a toroidal  $\lambda$  DNA condensate in the presence of  $\text{Co}(\text{NH}_3)_6^{3+}$ . The plane of the toroid is parallel to the image and the fringes represent DNA strands (obtained from ref. 48, copyright 2001 National Academy of Sciences, USA). (B) Average of 77 cryoelectron images of T7 bacteriophage heads from the complete tail-deletion mutant where DNA is compacted in a spool conformation perpendicular to the image plane and 2.5 nm spaced fringes of densely packed DNA are clearly visible (obtained with permission from ref. 53, copyright 1997, Elsevier). (C) T4 DNA compacted in the presence of poly(L-lysine)-covered silica nanoparticles 15  $\pm$  4 nm in diameter at a concentration of 5  $\times$  10<sup>-4</sup> wt%. Detail of DNA, dark line, wrapped around a single particle is shown on the left (obtained from ref. 14, copyright 2007, American Chemical Society). (D) Freeze-dried image of a chromatin fiber extracted from rat liver (obtained from ref. 54, © F. Thoma *et al.*, 1979. Originally published in *J. Cell Biol.*, **83**, 403–427.). Nucleosomes appear as dark circles linked by DNA lines.

been reported for tightly condensed DNA inside T7 virus capsids; a spool instead of a toroid is observed in this case<sup>53</sup> (Fig. 3B). When the compaction process is progressive, condensates are globular with a more disordered, liquid-like structure, although much less data are available.

The third mode of compaction depicted in Fig. 1 corresponds to the adsorption and wrapping of DNA around nanoscale objects. This mechanism, which is in play in the formation of the nucleosomes, is called complexation by some authors,<sup>59</sup> to distinguish it from pure compaction where the volume fraction of monomers in the condensed state is close to 1, while it is 10<sup>-2</sup> in the adsorption and wrapping mechanism and 10<sup>-5</sup> in a DNA random coil. This process is highly hierarchical and its elemental step is the wrapping of DNA around the nanoscale object. Many theoretical articles have addressed the complexation of DNA with nanoscale objects, as summarized in a comprehensive review by Schiessel.<sup>62</sup> The first and systematic experimental study was made by Zinchenko and coworkers<sup>13,14</sup> who studied the compaction of DNA in the presence of cationic nanoparticles of sizes ranging between 10 and 100 nm and monovalent salt concentrations spanning 10<sup>-2</sup> to 1 M. Three compaction modes were observed depending on the particle size: (i) adsorption of DNA on the particles larger than 40 nm; (ii) wrapping of DNA around particles of size 15 nm (Fig. 3C) in a way similar to chromatin (Fig. 3D) and (iii) adsorption of 10 nm particles onto

DNA.<sup>13,14</sup> The formation of the compact state for all nanoparticle sizes depended on the salt concentration in a similar way: low compaction at low and high salt concentrations and optimal compaction at intermediate salt concentrations.<sup>13,14</sup> This optimum is explained as the interplay between attractive and repulsive electrostatic interactions. At low salt, the increased rigidity of DNA due to the electrostatic contribution to the persistence length hinders compaction. At high salt,  $\kappa^{-1}$  becomes so small that the attractive electrostatic interaction between the DNA and the nanoparticles is screened. A similar salt effect is observed for the *in vitro* reconstitution of chromatin, *i.e.*, salt-induced complexation at intermediate salt concentration<sup>63</sup> and the salt-induced release of DNA from nucleosome core particles at high salt concentration.<sup>64</sup>

## 2.5. Control parameters of DNA compaction/decompaction

As discussed above, a variety of agents are able to induce the compaction of DNA. Here we discuss how physico-chemical parameters, such as salt concentration, solvent dielectric constant, temperature and other external stimuli, affect compaction and decompaction.

**(1) Increasing salt promotes compaction or decompaction.** In the presence of multivalent cations such as spermine, increasing mono- and divalent cation concentration induces decompaction.<sup>20</sup> This observation can be explained by an exchange equilibrium where multivalent cations adsorbed on DNA are displaced by low valency ones. On the contrary, in the presence of neutral polymers, such as polyethyleneglycol, increasing mono- and divalent cation ( $\text{Na}^+$ ,  $\text{Mg}^{2+}$ ) concentration promotes compaction.<sup>44,45</sup> In this case increasing salt enhances DNA electrostatic screening.

**(2) Increasing  $\epsilon_r$  promotes decompaction.** The electrostatic contribution to compaction is affected by the relative dielectric constant of the solvent,  $\epsilon_r$ .<sup>65</sup> This effect is well understood in the framework of the Manning–Oosawa condensation theory as a change in the Bjerrum length,  $l_B$ . DNA compaction in the presence of monovalent and divalent cations was observed when  $\epsilon_r$  was decreased using alcohol–water mixtures.<sup>20,43,66</sup> A similar effect is responsible for the increase in the compacting agent concentration at the onset of compaction with increasing  $\epsilon_r$ .<sup>21,22</sup>

**(3) Increasing temperature promotes compaction or decompaction.** When DNA is compacted by multi-valent counter-ions, such as spermine or  $\text{Co}(\text{NH}_3)_6^{3+}$ , increasing temperature promotes DNA compaction.<sup>67,68</sup> This is explained by the entropic contribution of free monovalent counter-ions that are more abundant in the compact state. On the contrary, this increase in counter-ions entropy promotes DNA unfolding when the compaction agent is a neutral polymer, such as polyethyleneglycol.<sup>69</sup>

**(4) An external perturbation that modifies the charge of the compaction agent allows one to control DNA compaction and decompaction.** When the valency of the compaction agent can be changed *in situ* by the action of an external stimulus, DNA compact and unfolded states are favoured for the high valency

and low valency forms, respectively. This has been demonstrated using a redox reaction on the couple  $\text{Fe}^{3+}/\text{Fe}^{2+}$ ,<sup>31</sup> through a pH variation applied in the presence of spermine,<sup>70</sup> or through complexation, reported with spermidine and ATP/ADP.<sup>71</sup> A similar perturbation was used on DNA compacted in the presence of cationic small unilamellar vesicles that were disrupted upon addition of a neutral surfactant leading to DNA decompaction.<sup>72</sup>

## 2.6. Reversible photocontrol of DNA compaction

A particularly interesting experimental parameter to control the compaction state of DNA is light because it is non-invasive and tunable in time and space. Photoreversible DNA condensation was first demonstrated by Le Ny and Lee in 2006.<sup>73</sup> They used a cationic surfactant carrying an azobenzene moiety, AzoTAB, standing for azobenzene trimethylammonium bromide, whose conformation changes upon illumination from a more hydrophobic *trans* isomer to a more hydrophilic *cis* form (Fig. 4). As a result, the affinity of the surfactant for DNA changes and DNA condensation could be tuned by light at constant AzoTAB concentration. This process is reversible and selective on the illumination wavelength: *trans* to *cis* isomerization occurred at 365 nm while *cis* to *trans* isomerization happened at 434 nm. We have later demonstrated that the compaction of T4-DNA with AzoTAB is a first order transition and that it is a suitable strategy for controlling single-molecule DNA conformation inside a biomimetic micro-environment using light.<sup>17</sup>

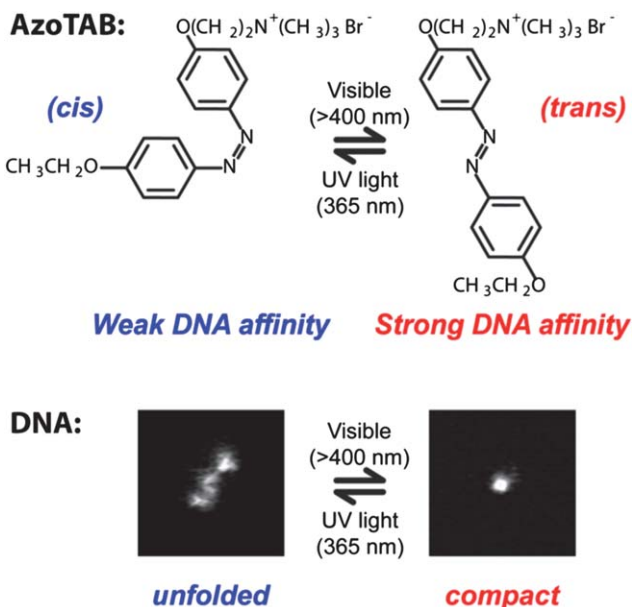


**Fig. 4** Azobenzene trimethylammonium bromide, AzoTAB, reversibly compacts DNA using light at two different wavelengths. Top: light illumination induces a *cis/trans* conformational transition that changes the dipolar moment of the surfactant resulting in a differential affinity for DNA. Bottom: DNA compaction can be tuned by light at constant AzoTAB concentration. Pictures are fluorescence microscopy images of an individual T4-DNA molecule stained with YOYO-1 in the presence of AzoTAB (700  $\mu\text{M}$ ) in 10 mM TE buffer, after visible (right) and UV (left) illumination. Image sizes are 5  $\mu\text{m} \times 5 \mu\text{m}$ .

The concentration of AzoTAB resulting in full DNA compaction was relatively high, typically 700  $\mu\text{M}$ , in these studies.<sup>17,73</sup> As a result, subsequent work has attempted to develop similar species with a lower critical compaction concentration. The picture that emerges is that increasing the hydrophobicity of the surfactant tail efficiently reduces this critical concentration, as demonstrated for gemini surfactants<sup>74</sup> and derivatives with an increasing number of methyl moieties,<sup>40</sup> but it also reduces the reversibility of the photoinduced decompaction. A good balance was achieved when the linker between the trimethylammonium and the azobenzene consisted of 5 (ref. 40) or 4 (ref. 75) methyl groups. These AzoTAB derivatives induced 100% compaction at 100 and 150  $\mu\text{M}$ , respectively, in 10 mM buffer. Moreover, two different approaches combining a cationic AzoTAB derivative and anionic species resulted in a significant decrease of the critical compaction concentration. Cationic vesicles with a net positive charge formed with an AzoTAB derivative and sodium dodecylbenzenesulfonate at concentrations of 48 and 19  $\mu\text{M}$ , respectively, were capable of the photoreversible condensation of DNA.<sup>76</sup> AzoTAB in the presence of 10<sup>-3</sup> wt% anionic silica nanoparticles reversibly compacted DNA at a concentration of 200  $\mu\text{M}$ .<sup>41</sup> In both cases, the decrease in the critical concentration was attributed to a cooperative effect induced by the anionic species that facilitates the aggregation of the cationic surfactant.

In addition to the reversibility of compaction it is important to consider the kinetics of the process, which of course depends on the photon flux. The photo-isomerization rate constant can be written as  $k = \epsilon I_0 \varphi$ , where  $\epsilon$  is the molar absorption coefficient at a given wavelength,  $I_0$  the radiative flux of light and  $\varphi$  the quantum yield of the photo-induced reaction. Typical values of  $\epsilon$  in the AzoTAB series are in the range  $1\text{--}3 \times 10^3 \text{ m}^2 \text{ mol}^{-1}$  and  $\varphi$ , measured for a triethyleneglycol derivative,<sup>77</sup> is about 1 and 0.7 for the *trans* to *cis* and *cis* to *trans* isomerizations, respectively. Photon fluxes of  $10^{-3}$  (mol of photons)  $\text{m}^{-2} \text{ s}^{-1}$  (corresponding to a 500 W Hg lamp) resulted in isomerization rates for an AzoTAB derivative of 3 and 2  $\text{s}^{-1}$  for the *trans* to *cis* and the *cis* to *trans* isomerizations, respectively.<sup>75</sup> These conditions resulted in the compaction and decompaction of 166 kbp long T4-DNA in 1 s without apparent DNA damage, indicating that the rate-limiting process is the DNA conformational transition.<sup>78</sup>

## 2.7. DNA origami

Although it is not usually considered a compaction technique, we would like to include here DNA origami as a sequence-directed strategy to obtain compact DNA structures. DNA origami consists of controlling the shape of a scaffold ssDNA several kbp long using hundreds of short ssDNA sequences as if they were staples that clamp two non-contiguous sequences of the scaffold backbone in a certain geometric configuration. Rothemund first proposed this idea and reported two-dimensional structures such as a smiley face and a map of the western hemisphere with a pixel size of 6 nm, with great reproducibility and relatively short folding times ( $\sim 1 \text{ h}$ ).<sup>79</sup> Later 3D nanoscale objects with diverse shapes were reported, for which much longer times, of the order of a week, were required for proper folding.<sup>80</sup> It is interesting to compare these very long assembly times to obtain the final

nanoscale object to the typical second-scale formation of toroids by unimolecular DNA compaction.

## 2.8. Summary on the fundamental aspects of DNA compaction

We saw that DNA compaction and decompaction can be controlled by a variety of physico-chemical stimuli. Table 1 summarizes for the main types of compaction agents the associated modes of compaction and the parameters that can be used to induce decompaction. Hereafter, we will focus on applications of DNA compaction/decompaction.

## 3. Reversible compaction for gene regulation

An important part of gene regulation in an organism occurs at the level of transcription and one can distinguish two principal strategies. On the one hand, a ligand (called a *trans* factor, such as a transcription factor or the bacterial  $\sigma$  factors) binds to a regulatory DNA sequence (*cis* element) and tunes the transcription activity of one or several genes in a sequence-dependent manner. On the other hand, the higher-order structure of the chromosome may modify the affinity of the *trans* factor or the RNA polymerase for the DNA sequence, by blocking its access for instance. This second strategy is expected to regulate gene activity over larger sets of genes and in a way that is less sensitive to the sequence. This structural influence on gene regulation has long ago been observed in the silencing properties of heterochromatin in eukaryotes<sup>85</sup> and its importance in bacteria has been revealed in the last decade:<sup>86,87</sup> supercoiling and DNA condensation play important roles in the regulation of gene expression.

The first to study the effect of DNA condensation on transcription were Baeza *et al.* in 1987.<sup>88</sup> They reported an enhancement of transcription in circular plasmids condensed with spermidine. Taking into account the low salt conditions of their experiments and the results described below we can now argue that their interpretation was probably wrong and the enhancement might have been due to spermidine–protein interactions. More recently, Tsumoto *et al.* demonstrated that the compaction of a 40 kbp long DNA, bearing a T7 promoter at half length, resulted in the sharp inhibition of transcriptional activity, using both spermine and PEG as compacting agents.<sup>89</sup> A comparable on/off switching of transcription due to compaction was very recently demonstrated in water-in-oil microdroplets coated with a phospholipid membrane using an elegant FRET assay for detecting single molecule mRNAs.<sup>90</sup> Results in a similar direction have been obtained when T4-DNA was complexed with cationic nanoparticles, although here the inhibition of

transcription with increasing concentration of nanoparticles was more gradual.<sup>91</sup>

## 4. Photocontrol of gene expression based on light-induced nucleic acid conformational changes

We have recently demonstrated that photocontrol of the compaction of nucleic acids (DNA, mRNA) allows to control gene expression *in vitro* using light at both transcription and translation levels<sup>92</sup> (Fig. 5 and 6). When AzoTAB is added to the gene expression system, DNA (respectively mRNA) folds and transcription (respectively translation) is switched off; after a short UV illumination (1–3 minutes at 365 nm), DNA (respectively mRNA) unfolds back and transcription (respectively translation) is switched on again.<sup>92</sup> We have demonstrated that this method is potentially applicable to any DNA template, regardless of its length (from 100 bp to 100 kbp) and its sequence, as well as to bacterial (*e.g.*, *E. coli*) or viral (*e.g.*, T7) polymerases. This method does not require any covalent modification of the substrates and it is reversible, which is an advantage over photo-uncaging strategies. In all cases, the compaction state of the nucleic acid correlated well with the level of RNA/protein produced. In the case of transcription, RNA production was inhibited by addition of AzoTAB and fully recovered upon UV illumination (Fig. 6A). Translation was also strongly reduced by AzoTAB and enhanced 3- to 6-fold by UV illumination (Fig. 6B). Moreover, this robust

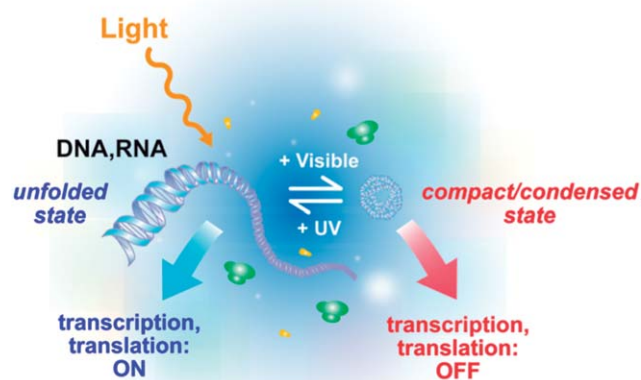


**Fig. 5** Schematic principle of the reversible photocontrol of gene activity (transcription and translation) based on light-induced DNA/RNA conformational changes.

**Table 1** Modes of compaction and possible decompaction method for various compaction agents

| Compaction agent                          | Mode of compaction                            | Decompaction                                                                                                                                                                                      |
|-------------------------------------------|-----------------------------------------------|---------------------------------------------------------------------------------------------------------------------------------------------------------------------------------------------------|
| Multivalent cation ( $3 \leq Z \leq 10$ ) | All-or-none <sup>11</sup>                     | [Salt] $\uparrow$ , <sup>20</sup> $T \downarrow$ , <sup>67,68</sup> $\varepsilon \uparrow$ , <sup>21,22,65</sup> $Z \downarrow$ ( <i>e.g.</i> , oxido-reduction, <sup>31</sup> pH <sup>70</sup> ) |
| Polycation ( $Z > 10$ )                   | Progressive <sup>12</sup>                     | Polyanions                                                                                                                                                                                        |
| Cationic nanoparticle                     | Adsorption and wrapping <sup>13,14</sup>      | [Salt] $\uparrow \downarrow$ <sup>13,14</sup>                                                                                                                                                     |
| Cationic surfactant                       | All-or-none + progressive <sup>16,17,39</sup> | Light, <sup>17,73</sup> adding cyclodextrine, <sup>81</sup> anionic <sup>82,83</sup> and non-ionic <sup>84</sup> surfactants                                                                      |
| Cationic vesicle                          |                                               | Adding detergent <sup>72</sup>                                                                                                                                                                    |
| Neutral polymer                           | All-or-none <sup>45</sup>                     | [Salt] $\downarrow$ , <sup>44,45</sup> $T \uparrow$ <sup>69</sup>                                                                                                                                 |

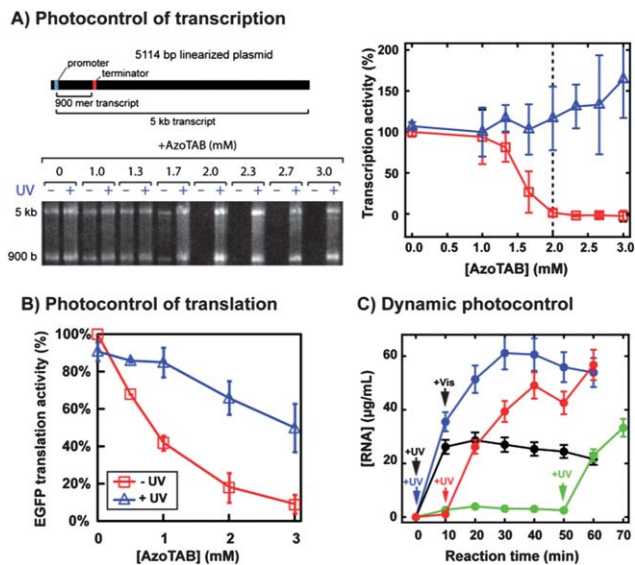


**Fig. 6** AzoTAB allows the reversible photocontrol of transcription and translation activity *in vitro*. (A) Production of RNA by *in vitro* transcription from a linearized plasmid coding for transcripts of two different lengths, 900 b and 5 kb at different AzoTAB concentrations, in the presence and in the absence of UV light (365 nm). Left, a denaturating RNA electrophoresis gel; right, normalized transcriptional activity. For  $[AzoTAB] \geq 2$  mM (dashed line), DNA is compacted and transcription is inhibited; upon UV illumination, DNA unfolds and transcription is recovered. (B) Normalized EGFP translation activity obtained in a cell-free *in vitro* expression system containing mRNA for different AzoTAB concentrations in the presence (blue triangles) and in the absence (red squares) of UV. (C) The production of RNA from a 144 bp dsDNA fragment condensed with 2 mM AzoTAB is dynamically controlled using light pulses that switch transcription ON (UV light) and OFF (visible light). Adapted from ref. 92.

approach allows dynamic ON and OFF photoswitches using sequential UV and visible illumination pulses, respectively (Fig. 6C). This is thus, to our knowledge, the only approach allowing both temporal and reversible control, in a sequence-independent way. By coupling this method to gene silencing using specific miRNAs, selective photocontrol was possible and the light-induced production of different combinations of a few target proteins was reported.<sup>93</sup> Lee and coworkers went a step forward and applied photoreversible DNA compaction to gene delivery inside mammalian cells.<sup>76</sup> In their *in vivo* studies, protein expression from an internalized plasmid increased 2-fold after UV illumination.

## 5. Compaction for protection

### 5.1. Protection against chemical or biochemical stress

In the unfolded state, genomic DNA is a very long molecule exposing a huge number of monomers (of the order of  $10^6$  in the case of human genomic DNA) to its physico-chemical micro-environment. In contrast, in the compact state DNA monomers are confined in a very dense state making them hardly accessible for other molecules present in the medium. For instance, it has been shown that in the toroidal condensate DNA is organized into a hexagonal array with an interhelix

spacing ranging between 2 and 3 nm,<sup>48,94–97</sup> leaving a free space between DNA consecutive rows that is smaller than 1 nm (DNA diameter is 2 nm). DNA monomers in such a highly packed structure are thus hardly accessible for surrounding chemical species. As a consequence, reversible DNA compaction can be used as a strategy to temporarily protect DNA from an external chemical or biochemical stress by applying the following procedure. In the absence of stress, DNA can be used in an unfolded and “reactive” state. Should a stress be applied, DNA can be folded into a compact and “silent” state and protected against reaction by stress molecules. When the stress is over, DNA unfolding allows recovering the initial “reactive” state. For instance, it has been shown that DNA compaction by multivalent metal cations ( $Al^{3+}$ ,  $Co^{3+}$ ),<sup>27</sup> short polyamines (mainly spermine (4+) and spermidine(3+))<sup>98,99</sup> and protamine<sup>100</sup> offers marked protection against fast neutron<sup>98</sup> or gamma ray<sup>99</sup> radiation-induced single- and double-strand DNA breakage, which has been explained by the reduced accessibility of DNA bases for radiation-induced reactive species.<sup>100</sup> Polyamines (mainly spermidine)<sup>101,102</sup> and protamine<sup>103</sup> have also regularly been used to protect DNA during the delivery into cells by bombardment. DNA compaction by spermidine is also known to inhibit DNA fragmentation by endonucleases, which prevents the onset of apoptosis.<sup>104</sup> Finally, DNA compaction by polyamines and analogs has been shown to offer marked protection against oxidative stress.<sup>105,106</sup>

### 5.2. Protection against mechanical stress

We saw that DNA compaction was a way to reversibly hide DNA monomers from their chemical environment and therefore to ensure protection against chemical and biochemical stresses. The dramatic change of DNA size upon compaction can also be exploited as a way to protect DNA against a mechanical stress. Basic manipulations, such as mixing, pipetting, or pumping/injecting, induce shear forces down to the characteristic Kolmogorov scale  $\eta$ , which is typically of the order of a few  $\mu m$ . According to the polymer-scission theory,  $\eta$  is both the minimal extended polymer length to get significant shear-induced chain scission and the size at which chain fragmentation occurs.<sup>107</sup> When unfolded genomic DNA molecules, which are much longer than  $\eta$ , are subjected to the above-mentioned manipulations, they thus experience intense molecular tension along their backbone and strong fragmentation into  $\mu m$  sized fragments. Reversible compaction, which brings each DNA molecule to an overall size much smaller than  $\eta$ , has been demonstrated to be a very efficient way to protect DNA against breakage by shearing stress (Fig. 7).<sup>108</sup> The protection against DNA breakage by compaction agent was reported for the first time by Kaiser *et al.*<sup>109</sup> and later confirmed by Cai *et al.*<sup>110</sup> and Kovacic *et al.*<sup>111</sup> The role of reversible folding transition in this protection effect was mentioned by Mizuno and Katsura<sup>112</sup> and precisely quantified by Cinque *et al.* who performed systematic DNA size measurements on tens of thousands of individual genomic molecules.<sup>108</sup> We can thus anticipate that the implementation of reversible DNA compaction strategies in biological protocols involving the manipulation of long DNA molecules shall greatly improve the feasibility and accuracy of analyses requiring the

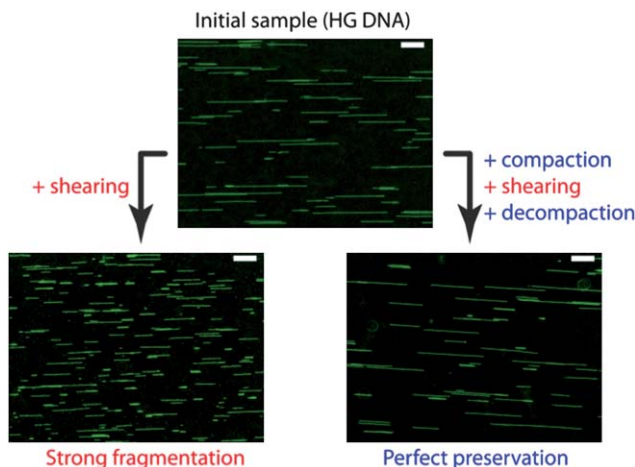


**Fig. 7** Example of DNA protection by compaction against mechanical stress. Human genomic (HG) DNA sample was submitted to controlled shear stress. Without compaction, molecules are strongly fragmented. If compaction is applied before shear stress, DNA molecules are perfectly preserved after shearing. Pictures are fluorescence images of individual HG DNA molecules combed on a silanized glass substrate. Scale bars are 10  $\mu$ m. Adapted from ref. 108.

preservation of genetic information contiguity, such as DNA mapping and chromosome rearrangement studies.<sup>108</sup>

## 6. Compact DNA as a nanostructure template

Unfolded DNA has been widely used as a template for nanostructure fabrication, enabling a broad variety of applications, as remarkably summarized in the recent review by Becerril and Woolley.<sup>113</sup> One of the strategies consists in the localization of transition metal cations through electrostatic interactions with and/or chelation by DNA bases prior to reduction to get a DNA-templated metallic nanostructure. Other involved interactions are  $\pi$ -stacking (DNA–organic molecule interaction) and DNA base pairing. Typical examples of DNA-templated realizations include synthesis of metal nanowires<sup>114,115</sup> and nanoparticle assembly on DNA scaffold.<sup>116,117</sup> Surprisingly, the use of compact DNA as a nanostructure template has been much less explored. This is all the more surprising that compact DNA offers readily available nanoscale shapes and organizations that can be very difficult to realize through classical strategies. This concept was demonstrated for the first time by Zinchenko *et al.* who used DNA compacted into toroids by spermine as templates for the one-pot synthesis of silver nanorings with a well-defined shape and size. Later, this strategy was used to produce palladium nanoparticles,<sup>118</sup> gold nanostructures,<sup>119</sup> and photoluminescent nanorings.<sup>120</sup> Because DNA-templated nanomaterial deposition can be applied to many atoms including Au,<sup>121</sup> Ag,<sup>114,122</sup> Pd,<sup>123</sup> Pt,<sup>124</sup> Cu,<sup>125,126</sup> Ni,<sup>127</sup> Co,<sup>128</sup> oxides such as Fe<sub>3</sub>O<sub>4</sub>,<sup>129</sup> and semi-conductors,<sup>130</sup> and due to the broad variety of nanoscale shapes that can be obtained either from unimolecular DNA compaction (toroids, rods, rackets, *etc.*) or using programmed assembly such as in the origami method, the use of compact DNA as a nanostructure template seems to be a strategy worth being developed and shall open the route to the controlled and programmed preparation of nanostructures with immense possibilities in terms of shape and composition.

## 7. Conclusions

In this review, we first provided a short physico-chemical description of DNA compaction (i) to provide essential fundamental understanding of the process which brings highly charged and semi-flexible DNA chain into a dense and highly organized nanostructure and (ii) to describe and rationalize the possible strategies to control DNA compaction and decompaction. For more details related to one or both of these aspects, other reviews might be consulted.<sup>3,5,6,56</sup> The fields of gene delivery and transfection, which are important applications of DNA compaction, were not described here but are well described in dedicated reviews.<sup>7</sup>

We saw that many strategies have been developed to control DNA compaction and decompaction. Among them, the most remarkable one is probably the photocontrol method initiated by Le Ny and Lee<sup>73</sup> and further developed by Baigl *et al.*<sup>17,40,74,92</sup> In this approach, without changing the chemical composition of DNA solution, DNA conformation can be controlled using light. In the presence of a photosensitive nucleic acid binder called AzoTAB, DNA is in a compact state under dark conditions. Upon UV illumination, DNA unfolds and stays in the unfolded state if kept in the dark. Upon visible illumination, DNA folds back to the compact state. This method has the great advantage to be reversible and several cycles of compaction/decompaction can be realized by successive visible/UV illuminations. Moreover, light is an ideal external trigger to control DNA conformation as it offers unique advantages: high spatio-temporal resolution of the excitation, tunability of the intensity, low perturbation of the biochemical environment, biocompatibility, and high potentiality for biotechnological applications.

In nature, DNA compaction has two main roles: packaging and regulation of gene expression. Transposed *in vitro*, we showed that these two properties can be declined in several kinds of applications (Fig. 8). In the process of DNA packaging, DNA

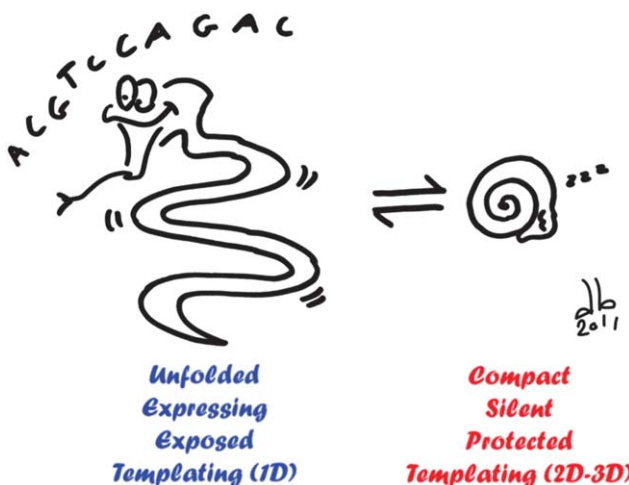


**Fig. 8** Schematic overview of possible applications of DNA compaction/decompaction. When DNA is unfolded (left), gene expression is activated, DNA is exposed to its environment and it can be used as a template for 1D nanostructure. When DNA is compacted (right), gene expression is silenced, DNA is protected over different biochemical and physical stresses and it can serve as a template for 2D and 3D nanostructures with a well-defined size and shape.

folds into highly organized and well-defined structures. On the one hand, because this is a reversible process, it can be used to reversibly protect DNA against mechanical, chemical, or biochemical stresses. Compaction-based protection of DNA has been mainly considered in fundamental studies. Implemented in biochemical protocols, it shall greatly improve the yield and precision of biological procedures such as genomic DNA extraction, manipulation, sequencing, and mapping.<sup>108</sup>

On the other hand, the well-defined morphologies of compact DNA (e.g., toroids, rods) can be used as templates to construct nanostructures with a well-defined size, shape, and composition.<sup>122</sup> Beside the naturally occurring DNA compact morphologies, a broad variety of shapes can be obtained by the origami method,<sup>79</sup> which considerably increases the variety of realizable templates in terms of shape, size, and spatial organization.

Finally, directly inspired by the natural role of DNA higher-order structure in gene regulation, DNA compaction can be used to control biochemical reactions involved in gene expression. This approach is particularly interesting when it is combined with the photocontrol method.<sup>92</sup> Very active research has been devoted in the past few years to the control of DNA transcription activity or gene expression by light.<sup>131</sup> Photocaged molecules have been widely and successfully applied but do not allow a reversible control.<sup>131</sup> Another strategy has been based on DNA modification with photoactivatable groups, which is hardly applicable to *in vivo* studies and requires specific chemical modification of DNA.<sup>132,133</sup> A third approach consists in the construction of a light-switchable gene promoter system, which has the advantage to be compatible *in vivo* but requires heavy gene construction protocols and is directed to one specific gene.<sup>134</sup> All these strategies are based on a sequence-dependent regulation and thus have to be adapted for each particular transcription/translation system. In contrast, by using light to control nucleic acid conformation, gene expression can be photocontrolled at both transcription and translation levels in a reversible and sequence-independent way.<sup>92</sup> This strategy shall find many applications for the dynamic photocontrol of gene expression of many kinds of machineries and target gene(s). The main remaining challenge is its implementation for *in vivo* and reversible photocontrol of gene expression.

## Notes and references

- 1 J. D. Watson and F. H. C. Crick, *Nature*, 1953, **171**, 737–738.
- 2 W. M. Gelbart, R. F. Bruinsma, P. A. Pincus and V. A. Parsegian, *Phys. Today*, 2000, **53**, 38–44.
- 3 V. A. Bloomfield, *Curr. Opin. Struct. Biol.*, 1996, **6**, 334–341.
- 4 V. A. Bloomfield, *Biopolymers*, 1997, **44**, 269–282.
- 5 A. Gonzalez-Perez and R. S. Dias, *Front. Biosci.*, 2009, **1**, 228–241.
- 6 A. Zinchenko, D. Baigl and K. Yoshikawa, in *Polymeric Nanostructures and Their Applications*, ed. H. S. Nalwa, American Scientific Publishers, Stevenson Ranch (CA), USA, 2007.
- 7 B. Demeneix, Z. Hassani and J.-P. Behr, *Curr. Gene Ther.*, 2004, **4**, 445–455.
- 8 N. Makita, M. Ullner and K. Yoshikawa, *Macromolecules*, 2006, **39**, 6200–6206.
- 9 G. S. Manning, *J. Chem. Phys.*, 1969, **51**, 924–933; F. Oosawa, in *Polyelectrolytes*, ed. M. Dekker, New York, 1971, ch. 5.
- 10 M. Takahashi, K. Yoshikawa, V. V. Vasilevskaya and A. R. Khokhlov, *J. Phys. Chem. B*, 1997, **101**, 9396–9401.
- 11 K. Yoshikawa, M. Takahashi, V. V. Vasilevskaya and A. R. Khokhlov, *Phys. Rev. Lett.*, 1996, **76**, 3029–3031.
- 12 T. Akitaya, A. Seno, T. Nakai, N. Hazemoto, S. Murata and K. Yoshikawa, *Biomacromolecules*, 2007, **8**, 273–278.
- 13 A. A. Zinchenko, K. Yoshikawa and D. Baigl, *Phys. Rev. Lett.*, 2005, **95**, 228101.
- 14 A. A. Zinchenko, T. Sakaue, S. Araki, K. Yoshikawa and D. Baigl, *J. Phys. Chem. B*, 2007, **111**, 3019–3031.
- 15 W. Chen, N. J. Turro and D. A. Tomalia, *Langmuir*, 2000, **16**, 15–19.
- 16 S. M. Mel'nikov, V. G. Sergeyev and K. Yoshikawa, *J. Am. Chem. Soc.*, 1995, **117**, 2401–2408.
- 17 M. Sollogoub, S. Guieu, M. Geoffroy, A. Yamada, A. Estevez-Torres, K. Yoshikawa and D. Baigl, *ChemBioChem*, 2008, **9**, 1201–1206.
- 18 Y. Yoshikawa, Y. S. Velichko, Y. Ichiba and K. Yoshikawa, *Eur. J. Biochem.*, 2001, **268**, 2593–2599.
- 19 K. Yoshikawa, Y. Yoshikawa, Y. Koyama and T. Kanbe, *J. Am. Chem. Soc.*, 1997, **119**, 6473–6477.
- 20 R. W. Wilson and V. A. Bloomfield, *Biochemistry*, 1979, **18**, 2192–2196.
- 21 P. G. Arscott, C. L. Ma, J. R. Wenner and V. A. Bloomfield, *Biopolymers*, 1995, **36**, 345–364.
- 22 D. Baigl and K. Yoshikawa, *Biophys. J.*, 2005, **88**, 3486–3493.
- 23 L. C. Gosule and J. A. Schellman, *Nature*, 1976, **259**, 333–335.
- 24 D. K. Chatteraj, L. C. Gosule and J. A. Schellman, *J. Mol. Biol.*, 1978, **121**, 327–337.
- 25 J. Widom and R. L. Baldwin, *J. Mol. Biol.*, 1980, **144**, 431–453.
- 26 J. Widom and R. L. Baldwin, *Biopolymers*, 1983, **22**, 1595–1620.
- 27 M. Spotheimmaurizot, F. Garnier, R. Sabattier and M. Charlier, *Int. J. Radiat. Biol.*, 1992, **62**, 659–666.
- 28 R. Ahmad, M. Naoui, J. F. Neault, S. Diamantoglou and H. A. TajmirRiahi, *J. Biomol. Struct. Dyn.*, 1996, **13**, 795–802.
- 29 H. A. TajmirRiahi, R. Ahmad and M. Naoui, *J. Biomol. Struct. Dyn.*, 1993, **10**, 865–877.
- 30 H. Arakawa, R. Ahmad, M. Naoui and H. A. Tajmir-Riahi, *J. Biol. Chem.*, 2000, **275**, 10150–10153.
- 31 Y. Yamasaki and K. Yoshikawa, *J. Am. Chem. Soc.*, 1997, **119**, 10573–10578.
- 32 U. K. Laemml, *Proc. Natl. Acad. Sci. U. S. A.*, 1975, **72**, 4288–4292.
- 33 R. S. Dias, A. Pais, M. G. Miguel and B. Lindman, *J. Chem. Phys.*, 2003, **119**, 8150–8157.
- 34 V. A. Kabanov, V. G. Sergeyev, O. A. Pyshkina, A. A. Zinchenko, A. B. Zezin, J. G. H. Joosten, J. Brackman and K. Yoshikawa, *Macromolecules*, 2000, **33**, 9587–9593.
- 35 C.-F. Ke, S. Hou, H.-Y. Zhang, Y. Liu, K. Yang and X.-Z. Feng, *Chem. Commun.*, 2007, 3374–3376.
- 36 M. W. Hsiang and R. D. Cole, *Proc. Natl. Acad. Sci. U. S. A.*, 1977, **74**, 4852–4856.
- 37 M. García-Ramírez and J. A. Subirana, *Biopolymers*, 1994, **34**, 285–292.
- 38 K. Hayakawa, J. P. Santerre and J. C. T. Kwak, *Biophys. Chem.*, 1983, **17**, 175–181.
- 39 R. Dias, S. Mel'nikov, B. Lindman and M. G. Miguel, *Langmuir*, 2000, **16**, 9577–9583.
- 40 A. Diguet, N. Mani, M. Geoffroy, M. Sollogoub and D. Baigl, *Chem. Eur. J.*, 2010, **16**, 11890–11896.
- 41 S. Rudiuk, K. Yoshikawa and D. Baigl, *Soft Matter*, 2011, DOI: 10.1039/c1sm05314k.
- 42 K. B. Roy, T. Antony, A. Saxena and H. B. Bohidar, *J. Phys. Chem. B*, 1999, **103**, 5117–5121.
- 43 S. M. Mel'nikov, M. O. Khan, B. Lindman and B. Jonsson, *J. Am. Chem. Soc.*, 1999, **121**, 1130–1136.
- 44 L. S. Lerman, *Proc. Natl. Acad. Sci. U. S. A.*, 1971, **68**, 1886–1890.
- 45 V. V. Vasilevskaya, A. R. Khokhlov, Y. Matsuzawa and K. Yoshikawa, *J. Chem. Phys.*, 1995, **102**, 6595–6602.
- 46 U. K. Laemml, J. R. Paulson and V. Hitchins, *J. Supramol. Struct.*, 1974, **2**, 276–301.
- 47 C. Conwell, I. D. Vilfan and N. V. Hud, *Proc. Natl. Acad. Sci. U. S. A.*, 2003, **100**, 9296–9301.
- 48 N. V. Hud and K. H. Downing, *Proc. Natl. Acad. Sci. U. S. A.*, 2001, **98**, 14925–14930.
- 49 V. V. Vasilevskaya, A. R. Khokhlov, S. Kidoaki and K. Yoshikawa, *Biopolymers*, 1997, **41**, 51–60.
- 50 P. G. Arscott, A. Z. Li and V. A. Bloomfield, *Biopolymers*, 1990, **30**, 619–630.
- 51 H. G. Hansma, *Annu. Rev. Phys. Chem.*, 2001, **52**, 71–92.
- 52 K. Yoshikawa, Y. Yoshikawa and T. Kanbe, *Chem. Phys. Lett.*, 2002, **354**, 354–359.

53 M. E. Cerritelli, N. Cheng, A. H. Rosenberg, C. E. McPherson, F. P. Booy and A. C. Steven, *Cell*, 1997, **91**, 271–280.

54 F. Thoma, T. Koller and A. Klug, *J. Cell Biol.*, 1979, **83**, 403–427.

55 N. Miyazawa, T. Sakae, K. Yoshikawa and R. Zana, *J. Chem. Phys.*, 2005, **122**, 4.

56 V. A. Bloomfield, *Biopolymers*, 1997, **44**, 269–282.

57 S. C. Riemer and V. A. Bloomfield, *Biopolymers*, 1978, **17**, 785–794.

58 R. Marquet and C. Houssier, *J. Biomol. Struct. Dyn.*, 1991, **9**, 159–167.

59 W. M. Gelbart, in *Electrostatic Effects in Soft Matter and Biophysics*, ed. C. Holm, P. Kekicheff and R. Podgornik, 2001, vol. 46, pp. 53–85.

60 M. R. Shen, K. H. Downing, R. Balhorn and N. V. Hud, *J. Am. Chem. Soc.*, 2000, **122**, 4833–4834.

61 P. Erbacher, T. Bettinger, P. Belguise-Valladier, S. M. Zou, J. L. Coll, J. P. Behr and J. S. Remy, *J. Gene Med.*, 1999, **1**, 210–222.

62 H. Schiessl, *J. Phys.: Condens. Matter*, 2003, **15**, R699.

63 E. C. Überbacher, V. Ramakrishnan, D. E. Olins and G. J. Bunick, *Biochemistry*, 1983, **22**, 4916–4923.

64 T. D. Yager, C. T. McMurray and K. E. Van Holde, *Biochemistry*, 1989, **28**, 2271–2281.

65 S. Flock, R. Labarbe and C. Houssier, *Biophys. J.*, 1996, **70**, 1456–1465.

66 M. Ueda and K. Yoshikawa, *Phys. Rev. Lett.*, 1996, **77**, 2133.

67 T. Saito, et al., *Europophys. Lett.*, 2005, **71**, 304.

68 D. Matulis, I. Rouzina and V. A. Bloomfield, *J. Mol. Biol.*, 2000, **296**, 1053–1063.

69 H. Mayama, T. Iwataki and K. Yoshikawa, *Chem. Phys. Lett.*, 2000, **318**, 113–117.

70 N. Makita and K. Yoshikawa, *Biophys. Chem.*, 2002, **99**, 43–53.

71 N. Makita and K. Yoshikawa, *FEBS Lett.*, 1999, **460**, 333–337.

72 A. Diguet and D. Baigl, *Langmuir*, 2008, **24**, 10604–10607.

73 A. L. M. Le Ny and C. T. Lee, *J. Am. Chem. Soc.*, 2006, **128**, 6400–6408.

74 M. Geoffroy, D. Faure, R. Oda, D. M. Bassani and D. Baigl, *ChemBioChem*, 2008, **9**, 2382–2385.

75 A.-L. M. Le Ny and C. T. Lee, Jr, *Biophys. Chem.*, 2009, **142**, 76–83.

76 Y.-C. Liu, A.-L. M. Le Ny, J. Schmidt, Y. Talmon, B. F. Chmelka and C. T. Lee, *Langmuir*, 2009, **25**, 5713–5724.

77 T. Shang, K. A. Smith and T. A. Hatton, *Langmuir*, 2003, **19**, 10764–10773.

78 K. Yoshikawa and Y. Matsuzawa, *J. Am. Chem. Soc.*, 1996, **118**, 929–930.

79 P. W. K. Rothmund, *Nature*, 2006, **440**, 297–302.

80 S. M. Douglas, H. Dietz, T. Liedl, B. Hogberg, F. Graf and W. M. Shih, *Nature*, 2009, **459**, 414–418.

81 A. González-Pérez, J. Carlstedt, R. S. Dias and B. Lindman, *Colloids Surf. B*, 2010, **76**, 20–27.

82 S. Bhattacharya and S. S. Mandal, *Biochemistry*, 1998, **37**, 7764–7777.

83 R. S. Dias, B. Lindman and M. G. Miguel, *J. Phys. Chem. B*, 2002, **106**, 12608–12612.

84 R. S. Dias, J. Innerlohinger, O. Glatter, M. G. Miguel and B. Lindman, *J. Phys. Chem. B*, 2005, **109**, 10458–10463.

85 E. J. Richards and S. C. R. Elgin, *Cell*, 2002, **108**, 489–500.

86 D. F. Browning and S. J. W. Busby, *Nat. Rev. Microbiol.*, 2004, **2**, 57–65.

87 S. C. Dillon and C. J. Dorman, *Nat. Rev. Microbiol.*, 2010, **8**, 185–195.

88 I. Baeza, P. Gariglio, L. M. Rangel, P. Chavez, L. Cervantes, C. Arguello, C. Wong and C. Montanez, *Biochemistry*, 1987, **26**, 6387–6392.

89 K. Tsumoto, F. Luckel and K. Yoshikawa, *Biophys. Chem.*, 2003, **106**, 23–29.

90 A. Tsuji and K. Yoshikawa, *J. Am. Chem. Soc.*, 2010, **132**, 12464–12471.

91 A. A. Zinchenko, F. Luckel and K. Yoshikawa, *Biophys. J.*, 2007, **92**, 1318–1325.

92 A. Estevez-Torres, C. Crozatier, A. Diguet, T. Hara, H. Saito, K. Yoshikawa and D. Baigl, *Proc. Natl. Acad. Sci. U. S. A.*, 2009, **106**, 12219–12223.

93 S. Rudiuk, H. Saito, T. Hara, T. Inoue, K. Yoshikawa and D. Baigl, submitted.

94 M. Suwalsky, W. Traub, U. Shmueli and J. A. Subirana, *J. Mol. Biol.*, 1969, **42**, 363.

95 T. Maniatis, J. H. Venable and L. S. Lerman, *J. Mol. Biol.*, 1974, **84**, 37.

96 D. C. Rau and V. A. Parsegian, *Biophys. J.*, 1992, **61**, 246–259.

97 J. A. Schellman and N. Parthasarathy, *J. Mol. Biol.*, 1984, **175**, 313–329.

98 M. Spotheimmaurizot, S. Ruiz, R. Sabattier and M. Charlier, *Int. J. Radiat. Biol.*, 1995, **68**, 571–577.

99 G. L. Newton, J. A. Aguilera, J. F. Ward and R. C. Fahey, *Radiat. Res.*, 1996, **145**, 776–780.

100 M. Suzuki, C. Crozatier, K. Yoshikawa, T. Mori and Y. Yoshikawa, *Chem. Phys. Lett.*, 2009, **480**, 113–117.

101 T. M. Klein, E. D. Wolf, R. Wu and J. C. Sanford, *Nature*, 1987, **327**, 70–73.

102 A. Perl, H. Kless, A. Blumenthal, G. Galili and E. Galun, *MGG, Mol. Gen. Genet.*, 1992, **235**, 279–284.

103 E. Sivamani, R. K. DeLong and R. D. Qu, *Plant Cell Rep.*, 2008, **28**, 213–221.

104 B. Brune, P. Hartzell, P. Nicotera and S. Orrenius, *Exp. Cell Res.*, 1991, **195**, 323–329.

105 A. U. Khan, Y. H. Mei and T. Wilson, *Proc. Natl. Acad. Sci. U. S. A.*, 1992, **89**, 11426–11427.

106 I. Nayvelt, M. T. Hyvonen, L. Alhonen, I. Pandya, T. Thomas, A. R. Khomutov, J. Vepsalainen, R. Patel, T. A. Keinanen and T. J. Thomas, *Biomacromolecules*, 2010, **11**, 97–105.

107 S. A. Vanapalli, S. L. Ceccio and M. J. Solomon, *Proc. Natl. Acad. Sci. U. S. A.*, 2006, **103**, 16660–16665.

108 L. Cinque, Y. Ghomchi, Y. Chen, A. Bensimon and D. Baigl, *ChemBioChem*, 2010, **11**, 340–343.

109 D. Kaiser, C. W. Tabor and H. Tabor, *J. Mol. Biol.*, 1963, **6**, 141.

110 W. W. Cai, H. Aburatani, V. P. Stanton, D. E. Housman, Y. K. Wang and D. C. Schwartz, *Proc. Natl. Acad. Sci. U. S. A.*, 1995, **92**, 5164–5168.

111 R. T. Kovacic, L. Comai and A. J. Bendich, *Nucleic Acids Res.*, 1995, **23**, 3999–4000.

112 A. Mizuno and S. Katsura, *Journal of Biological Physics*, 2002, **28**, 587–603.

113 H. A. Becerril and A. T. Woolley, *Chem. Soc. Rev.*, 2009, **38**, 329–337.

114 E. Braun, Y. Eichen, U. Sivan and G. Ben-Yoseph, *Nature*, 1998, **391**, 775–778.

115 A. Ongaro, F. Griffin, L. Nagle, D. Iacopino, R. Eritja and D. Fitzmaurice, *Adv. Mater.*, 2004, **16**, 1799.

116 H. Nakao, H. Shiigi, Y. Yamamoto, S. Tokonami, T. Nagaoka, S. Sugiyama and T. Ohtani, *Nano Lett.*, 2003, **3**, 1391–1394.

117 G. Wei, H. L. Zhou, Z. G. Liu, Y. H. Song, L. Wang, L. L. Sun and Z. Li, *J. Phys. Chem. B*, 2005, **109**, 8738–8743.

118 Y. Hatakeyama, M. Umetsu, S. Ohara, F. Kawadai, S. Takami, T. Naka and T. Adschar, *Adv. Mater.*, 2008, **20**, 1122.

119 T. C. Preston and R. Signorell, *Langmuir*, 2010, **26**, 10250–10253.

120 Y. Z. You, Z. Q. Yu, M. M. Cui and C. Y. Hong, *Angew. Chem., Int. Ed.*, 2010, **49**, 1099–1102.

121 A. Ongaro, F. Griffin, P. Beeher, L. Nagle, D. Iacopino, A. Quinn, G. Redmond and D. Fitzmaurice, *Chem. Mater.*, 2005, **17**, 1959–1964.

122 A. A. Zinchenko, K. Yoshikawa and D. Baigl, *Adv. Mater.*, 2005, **17**, 2820.

123 J. Richter, R. Seidel, R. Kirsch, M. Mertig, W. Pompe, J. Plaschke and H. K. Schackert, *Adv. Mater.*, 2000, **12**, 507.

124 R. Seidel, L. C. Ciacci, M. Weigel, W. Pompe and M. Mertig, *J. Phys. Chem. B*, 2004, **108**, 10801–10811.

125 C. F. Monson and A. T. Woolley, *Nano Lett.*, 2003, **3**, 359–363.

126 A. Rotaru, S. Dutta, E. Jentszsch, K. Gothelf and A. Mokhir, *Angew. Chem., Int. Ed.*, 2010, **49**, 5665–5667.

127 H. A. Becerril, P. Lutdk, B. M. Willardson and A. T. Woolley, *Langmuir*, 2006, **22**, 10140–10144.

128 Q. Gu, C. D. Cheng and D. T. Haynie, *Nanotechnology*, 2005, **16**, 1358–1363.

129 D. Nyamjav and A. Ivanisevic, *Biomaterials*, 2005, **26**, 2749–2757.

130 A. Houlton, A. R. Pike, M. A. Galindo and B. R. Horrocks, *Chem. Commun.*, 2009, 1797–1806.

131 G. Mayer and A. Heckel, *Angew. Chem., Int. Ed.*, 2006, **45**, 4900–4921.

132 M. Z. Liu, H. Asanuma and M. Komiyama, *J. Am. Chem. Soc.*, 2006, **128**, 1009–1015.

133 A. Rotaru and A. Mokhir, *Angew. Chem., Int. Ed.*, 2007, **46**, 6180–6183.

134 S. Shimizu-Sato, E. Huq, J. M. Tepperman and P. H. Quail, *Nat. Biotechnol.*, 2002, **20**, 1041–1044.